

## Scour due to Offset Jets

### **Dr. Rajashree Lodh**

BE (Civil) (TIT, Tripura), ME (Civil) (BESU, Shibpur), PhD (Civil) (IIT Kharagpur)  
Assistant Professor, Heritage Institute of Technology, Kolkata, West Bengal, INDIA, and  
Post-doctoral Researcher,  
MultiSpectra Consultants,  
23, Biplabi Ambika Chakraborty Sarani,  
Kolkata – 700029, West Bengal, INDIA.  
E-mail: shree1504@gmail.com

### **Dr. Amartya Kumar Bhattacharya**

BCE (Hons.) ( Jadavpur ), MTech ( Civil ) ( IIT Kharagpur ), PhD ( Civil ) ( IIT Kharagpur ),  
Cert.MTERM ( AIT Bangkok ), CEng(I), FIE, FACCE(I), FISH, FIWRS, FIPHE, FIAH, FAE, MIGS,  
MIGS – Kolkata Chapter, MIGS – Chennai Chapter, MISTE, MAHI, MISCA, MIAHS, MISTAM,  
MNSFMFP, MIIBE, MICI, MIEES, MCITP, MISRS, MISRMTT, MAGGS, MCSI, MIAENG, MMBSI,  
MBMSM  
Chairman and Managing Director,  
MultiSpectra Consultants,  
23, Biplabi Ambika Chakraborty Sarani,  
Kolkata – 700029, West Bengal, INDIA.  
E-mail: dramartyakumar@gmail.com

## **CONTENTS**

### **1 Introduction**

- 1. General  
1
- 1. Scope of this Work  
2
- References

### **2 Turbidity Currents**

- 2. General  
1
- 2. Review of Literature  
2
- 2. Velocity Distribution  
3
- 2. Concentration Distribution  
4
- 2. Conclusion  
5
- References

### **3 Scour due to Offset Jets**

- 3. General  
1
- 3. Review of Literature  
2
- 3. Parameters Related to Scour  
3
- 3. Experimental Setup and Procedure  
4
- 3. Scouring Process  
5
- 3. Scour Profiles  
6

3.  
7 **Distributions of Velocity Profiles**

3.  
8 **Conclusions**

**References**

# 1

## Introduction

### 1.1 General

India's water resources become increasingly strained, as the population of India continues to expand. Discharge of untreated sewage is the single most important cause for pollution of surface and ground water in India. Heavy pollution from open sewers is common place in urban areas and arsenic contamination of groundwater continues to threaten the health and well-being of local communities. India is defined as a 'water stressed' country and innovative methods to provide cost-effective water treatment to communities are a crucial requirement if growing populations are to be sustainable. Sewage are to be removed by applying different sewage treatments. A natural river continually picks up waste products from and drops them on its bed throughout its course. Knowledge of sediment transport can be applied extensively in civil engineering such as to plan how to control the flow of water in culverts, over spillways, below pipelines and around bridge piers and abutments, excess of which can damage the environment and failure of foundation of the structures. Moreover, when suspended load of sediment is substantial due to human activities, it can cause environmental hazards including filling up of the channels by siltation. Sediment transport is the movement of organic and inorganic particles by water. In general, the greater the flow, the more sediment will be conveyed. Water flow can be strong enough to suspend particles in the water column as they move downstream, or simply push them along the bottom of a waterway. Transported sediment may include mineral matter, chemicals and pollutants, and organic material. The total load includes all particles moving as bed load, suspended load, and wash load.

Turbidity, as an optical property of water, is one of the more difficult parameters to measure. Turbidity is caused by particles and coloured material in water. Total suspended solids (TSS) are the main cause of turbidity. Turbidity currents are most

typically underwater currents of usually rapidly moving, sediment-laden water moving down a slope. Turbidity currents can also occur in other fluids besides water. In the most typical case of oceanic turbidity currents, sediment laden waters situated over sloping ground flow down-hill because they have a higher density than the adjacent waters. The driving force behind a turbidity current is gravity acting on the high density of the sediments temporarily suspended within a fluid. As such currents flow, they often have a "snow-balling-effect", as they stir up the ground over which they flow, and gather even more sedimentary particles in their current. Their passage leaves the ground scoured and eroded. Once a turbidity current reaches the calmer waters of the flatter area, the particles borne by the current settle out of the water column. The sedimentary deposit of a turbidity current is called a turbidite. When sediment transport removes material from a streambed or bank, the erosion process is called scour. Scour can occur anywhere where there is water flow and erodible material. Local scour is an engineering term for the isolated removal of sediment at one location, such as the base of underwater structures, including bridge piers and abutments. This localized erosion can cause structural failure, as bridges and overwater constructions rely on the bed sediment to support them.

## **1.2 Scope of this work**

The objective of the present work is to understand the hydrodynamics of turbidity currents over plane beds based on velocity and concentration distributions. The sewage can be removed by offset jets and a special attempt is made on the scouring process using offset jets.

## **References**

- Dey, S. (2014). *Fluvial Hydrodynamics: Hydrodynamic and Sediment Transport Phenomena*, Springer, Berlin.
- Metcalf, L., Eddy, H. P. (1922). *Sewerage and Sewage Disposal: A Textbook*. New York: McGraw-Hill.

# 2

## Turbidity Currents

### 2.1 General

*Turbidity currents* are density currents that are generated due to the density difference of suspended sediments and water in a mixture. In turbidity currents, suspended sediment makes the density of the mixture greater than the density of the ambient water and provides the driving force; the sediment laden flow must generate enough turbulence to hold the sediment in suspension. They can be observed in the flows entering large bodies of water containing high concentration of suspended sediments. These are sediment-laden gravity currents that exchange sediment with the bed by erosion or deposition as the flow travels over the down slope. Turbidity currents derive this driving force from the sediment in suspension. They experience a resisting shear force on the bed and entrain water from above. Two types of turbidity currents can be distinguished: Low velocity, low density and high velocity, high density. High velocity, high density turbidity currents often carry suspended materials introduced near the shore to the deep sea.

Turbidity currents can be originated by various processes. Discharges of large amounts of sediments, e.g., mine tailings, underwater landslides caused by earthquakes, and re-suspension of suspended materials by waves during storms are three possibilities. Turbidity currents can be eroding or depositing, accelerating or decelerating, depending on the combination of initial conditions, bed slope, and size of sediment particles. A turbidity current with deposition and erosion is a flow in three components: clear ambient water, turbid water and sediment (bed material). The turbidity current entrains clear water into the flow and simultaneously either deposits suspended sediment on the channel bed, or entrains bed material into the flow. Actually turbidity current entrains and deposits at the same time, but there is a net flux either to the bed (depositing current) or from the bed (entraining current). Turbidity currents are self-generated

currents. The flow will vanish when all suspended materials are deposited on the bottom, and grow when sediments are entrained from the bed.

Turbidity current is made up of a front or head advancing into the ambient fluid, being followed by the body. The driving force for the front (unsteady flow) is the pressure gradient which is due to the density difference between the front and the ambient fluid. The driving force for body (steady flow) is the gravitational force of the heavier fluid. A schematic diagram of turbidity current is shown in Fig. 2.1.

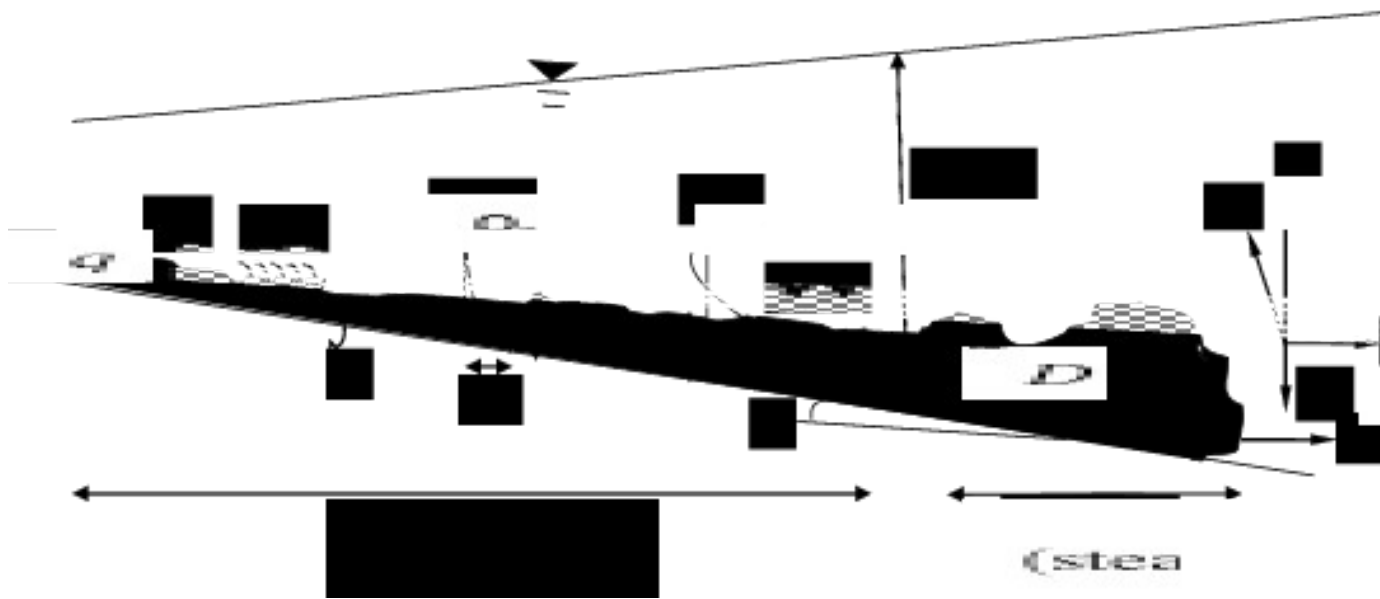


**Fig. 2.1** Definition sketch of turbidity current

## 2.2 Review of Literature

The characteristics and behaviour of turbidity currents was studied by many investigators and some of them are reviewed below.

Akiyama and Stefan (1985) derived various equations that govern the movement of two-dimensional gradually varied turbidity currents in reservoirs and over beaches and solved numerically. The model included and quantified all mechanisms which control accelerating and decelerating turbidity currents. The model consisted of depth-integrated equations for conservation of mass and volume, momentum equations and an empirical relationship for water entrainment and sediment entrainment. The equations were numerically solved by a Runge-Kutta method. The flow of turbidity current was found to be dependent on three factors: initial conditions, the size of the suspended sediment particles and the channel slope. The model explained clearly the differences as well as the similarities between subsurface gravity currents with and without sediment erosion and deposition. Parker et al. (1986) presented a general concept of the equations of motion of turbidity currents, their closure, and their solution for the continuous, spatially developing case in submarine canyons. Special attention is drawn on the possibility of self-acceleration, or ignition, by means of the incorporation of bed sediment into the current. Two models are presented. The first of these is the three-equation model, which can be considered as a generalization of the model of Ellison and Turner (1959) for simple, conservative density currents to the case of eroding and depositing turbidity currents. The self-acceleration predicted by the three-equation model was so strong that the energy constraint failed to be satisfied. The problem was rectified by the formulation of a four-equation model, in which an explicit accounting was made of the mean energy of the turbulence. Sediment entrainment from the bed was linked to the level of turbulence in the four-equation model. Parker et al. (1987) conducted various experiments to determine the behaviour of turbidity currents laden with non-cohesive silt (silica flour) moving down a slope the bed of which was covered with similar silt. The motion of the head was not studied; measurements were concentrated on the continuous part of the current that was essentially constant in time but developing in space. Only supercritical currents were studied. The currents were free to erode sediment from and deposit sediment on the bed. Experimental data were used to establish approximate similarity laws for the velocity and concentration

distribution, and to evaluate several shape factors that enter in the vertically-integrated equations of motion. Stacey and Bowen (1988) developed a simple numerical model that successfully simulated observations of small-scale, laboratory, density currents flowing down inclines of constant slope. The model results suggested that laboratory determinations of the bulk Richardson number have been biased by molecular processes but that determinations of the entrainment coefficient are probably applicable to large scale currents, and even to turbidity currents in which the gravitational driving force is provided by suspended sediment. The entrainment coefficient as a function of bottom slope is accurately simulated by the model down to slopes as small as 0.5 degree. Its value depends primarily on the stability of the current above the velocity maximum, which is not a function of the drag coefficient. Garcia (1993) conducted laboratory experiments to study the behaviour of turbidity currents in the proximity of a slope transition. Saline currents and sediment laden currents (which included two grades of silica and two grades of glass beads) were generated and the hydraulic jumps showed similar characteristics. During experiments, several velocity profiles were measured and plotted which showed a distribution resembling that of a wall jet. Altinakar et al. (1996) presented a series of experiments with turbidity currents using two different types of sediments and those experiments were supplemented by saline gravity currents. The sediments used were fine, K-13 ( $d_s = 0.047$  mm) and the coarse, K-06 ( $d_s = 0.026$  mm) sediments of specific gravity 2.65. The velocity distributions for all runs were evaluated and plotted. The turbidity current can be divided into two regions: wall region (turbulence is created by bottom shear and sediment entrainment) and jet region (turbulence is created by free shear zone and water entrainment). The height,  $h$  where the velocity is maximum,  $u = U_m$  separates these regions. The velocity distribution in the wall region is expressed by logarithmic relation Eq. 2.1 or an empirical power relation Eq. 2.2 which when plotted gives an experimental value of  $n = 1/6$ . The distribution in the jet region is represented by a near-Gaussian relation given by Eq. 2.3. If the exponent is taken to be constant,  $m = 2$ , a curve fitted to the whole data set yields,  $\alpha_c = 1.412 \pm 0.065$ .

$$\frac{u(z)}{U_m} = \frac{1}{k} \ln z + c \quad (2.1)$$

$$\frac{u(z)}{U_m} = \left( \frac{z}{h_m} \right)^n \quad (2.2)$$

$$\frac{u(z)}{U_m} = \exp \left[ -a_c \left( \frac{z-h_m}{h-h_m} \right) \right] \quad (2.3)$$

where,  $h$  and  $U$  are the height and velocity of the current.

Lee and Yu (1997) studied the hydraulic characteristics of the turbidity current in a reservoir by a series of experiments. Kaolin was used as the suspended material. The plunge points were found to be unstable initially. As the experiment went on, it moved downstream from the incipient plunge location and finally reached a stable location. The thickness of the turbidity current was found to increase while the layer-averaged velocity and concentration decrease in the longitudinal direction, the layer-averaged velocity has the smallest variation rates. Equations for the dimensionless velocity and concentration profiles were obtained. A layer with approximately constant concentration, named denser layer, was observed in the study. Sequeiros et al. (2010) presented results of a set of 74 experiments that focus on the characteristics of velocity and fractional excess density profiles of saline density and turbidity currents flowing over a mobile bed of loose granular particles. The parameters that were varied during the experiments included flow discharge, fractional excess density, bed material, and bottom slope. The profiles were plotted and analysed. Experimental data were used to establish similarity relations for vertical profiles of velocity and fractional excess density, and to evaluate shape factors used in the depth-averaged equations of motion for different flow and bed conditions.

### 2.3 Velocity Distribution

The velocity distribution in turbidity current in a fully developed state is almost similar to that in submerged plane wall jet. A submerged plane wall jet is described as a jet of fluid that impinges tangentially (or at an angle) on a solid wall surrounded by the same fluid (stationary or moving) progressing along the wall (Dey et al., 2010). For a turbidity current, on one side (in the inner layer), the current is confined to the bed, while on the other side (in the outer layer), it is bounded by the stationary ambient fluid (Fig. 2.1). The boundary conditions for the velocity distribution in turbidity current are such that the velocity vanishes at the bed and at the interface between the turbidity current and the ambient fluid. Thus, the velocity distribution attains a maximum (peak velocity) at

the extremity of the inner layer, that is, the junction of the inner and outer layers of the current. Below the maximum velocity level (in the inner layer), the flow is characterized by a boundary layer flow, while above the maximum velocity level (in the outer layer), the flow is structurally similar to a free jet. Therefore, the turbidity currents are composed of an inner shear layer influenced by the bed and an outer layer of the self-similar type of a shear flow (Parker et al., 1987; Stacey and Bowen, 1988; Altinakar et al., 1996).

The datasets in the form of non-dimensional stream-wise distance  $z/\delta$  over non-dimensional velocity  $u(z)/U_m$  are plotted and a comparison is made with the plots of Altinakar et al. (1996), Garcia (1993) and Sequeiros et al. (2010). The inner layer and outer layer of jet refer to the zones below and above the point of occurrence of maximum velocity  $U_m$ , called the jet velocity. Precisely, the jet layer ( $\eta > \eta_0$ ) extends up to the inflection point (that is, the point of change of sign of slope ( $d^2u/dz^2$ ) of a  $u$ -distribution. Below the jet layer, there exists a wall region layer ( $\eta \leq \eta_0$ ). The jet layer thickness  $\delta$  is important from the viewpoint of scaling the vertical distance  $z$  (Dey et al. 2010).  $\eta_0$  refers to the ratio of  $z_0$  (the distance from the bed where the maximum velocity occurs) to jet layer thickness  $\delta$  and  $\eta$  refers to the ratio of  $z$  (any distance above the point of occurrence of maximum velocity) to the jet layer thickness  $\delta$ .

In the near-boundary zone (that is, within the inner layer of the jet) ( $\eta \leq \eta_0$ ), the  $1/m$ -th power law is assumed which is found to fit well for the datasets.

$$\frac{u(z)}{U_m} = \frac{1}{m} \left( \frac{\eta}{\eta_0} \right)^{\frac{1}{m}} \left( 1 + m - \frac{\eta}{\eta_0} \right) \quad (2.4)$$

In the jet region,  $\eta > \eta_0$ , boundary effects come into account and the following relation given by (Dey et al. 2010) holds well.

$$\frac{u(z)}{U_m} = \sec h^2 (\eta - \eta_0) [1 + \alpha \tanh (\eta - \eta_0)] \quad (2.5)$$

where  $\alpha$  is an additional term mainly due to submergence.

The values of  $m$  and  $\alpha$  are calculated for all velocity profiles of experimental data and averaged. The values that gives better degree of accuracy is  $m = 1/2$  and  $\alpha = -1.036$  obtained by using  $\eta_0 = 0.25$  and  $\delta = 1$ , which are contradictory to the results obtained by

Altinakar et al., (1996), i.e.,  $m = 1/6$  and  $\alpha = 1.4$ . Moreover, whether the value of  $m$  obtained is accurate or not has also been tested by power law in a different form and third-order polynomial law as,

$$\frac{u(z)}{U_m} = \zeta^{\frac{1}{m}} \quad (2.6)$$

$$\frac{u(z)}{U_m} = 1.5\zeta - 0.5\zeta^3 \quad (2.7)$$

The distance at which inflection point occurs can be obtained by equating Eq. 2.5 to zero,

$$\operatorname{sech}^2(\eta - \eta_0) [1 + a \tanh(\eta - \eta_0)] = 0 \quad (2.8)$$

Putting the values of  $\alpha$  and  $\eta_0$ ,

$$1 - 1.036 \tanh(\eta - 0.25) = 0$$

$$\eta = \eta_{\max} = 2.2676 \quad (2.9)$$

The dimensionless discharge is calculated as below

$$q = \int_{\eta_0}^{\eta_1} \frac{u(z)}{U_m} d\eta + \int_0^{\eta_{\max}} \frac{u(z)}{U_m} d\eta \quad (2.10)$$

$$= \int_0^{\eta_0} \left[ \frac{1}{m} \left( \frac{\eta}{\eta_0} \right)^{\frac{1}{m}} \left( 1 + m \frac{\eta}{\eta_0} \right) \right] d\eta + \int_{\eta_0}^{\eta_{\max}} [\operatorname{sech}^2(\eta - \eta_0) \{1 + a \tanh(\eta - \eta_0)\}] d\eta$$

Solving, we get

$$q = 0.67 \quad (2.11)$$

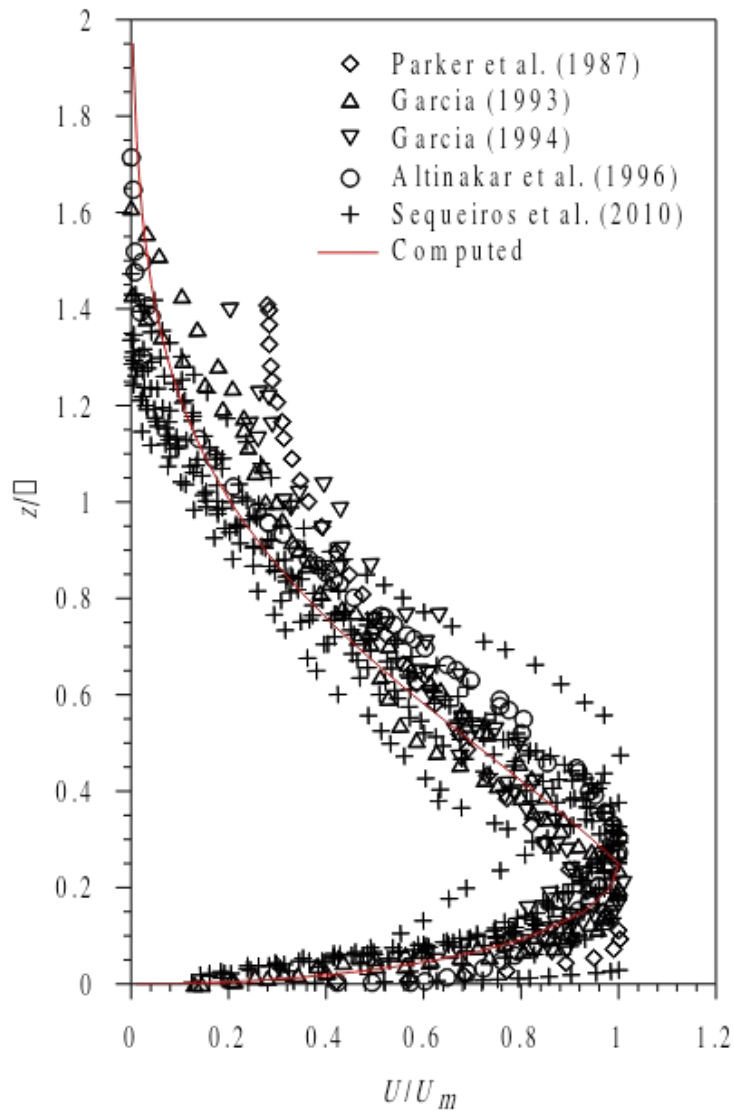


**Fig. 2.2** Computed dimensionless velocity profiles

Fig. 2.2 displays the computed velocity distributions obtained from Eq. 2.4 and 2.5. The experimental data plots of turbidity and salinity currents obtained from Parker et al. (1987), García (1993,1994), Altinakar et al. (1996), Sequeiros et al. (2010) are overlapped on the computed curves in Fig. 2.2 for comparison.

#### **2.4 Concentration distribution**

The turbidity current can be considered as a self-generated current in which sediment particles are suspended by the turbulence. The transport of suspended sediment particles in turbulent flow takes place due to the advection and diffusion processes in the ambient fluid.

The concentration distribution is given:

In the near boundary zone ( $\eta \leq \eta_0$ ), by a Rousean relation as

$$\frac{c}{C_0} = \exp\left(-w_s \int_{\eta_0}^{\eta} \frac{d\eta}{\xi_s}\right) \quad (2.12)$$

where  $C_0$  is the reference concentration at a distance of  $\eta_0 = 0.25$  from the bed where the velocity is maximum,  $w_s$  is the settling velocity of the particles and  $\xi_s$  is the diffusivity of sediment particle given as a function of  $\eta$  as

$$\xi_s = \beta k u_* \eta \left(1 - \frac{\eta}{\eta_0}\right)^m \quad (2.13)$$

where  $k$  is the von Kármán constant,  $u_*$  is the bed shear velocity, a coefficient  $\beta = 1$  (Rouse, 1937) and  $m$  is a coefficient taken as 0.9.

Integrating Eq. 2.12 by inserting Eq. 2.13, the following expression is obtained:

$$\frac{c}{C_0} = e^{-\zeta \int \left(1 - \frac{\eta}{\eta_0}\right)^m d\eta} \quad (2.14)$$

$\zeta = w_s / \beta k u_*$  which is called the Rouse number.

In the jet region,  $\eta > \eta_0$ , by a Rousean relation:

$$\frac{c}{C_0} = \exp\left(-\zeta \frac{\eta - \eta_0}{\eta_{\max}}\right)^{\lambda_c} \quad (2.15)$$

$$\varepsilon_s = \beta k u_* \frac{1}{\lambda_c} (\eta - \eta_0) \left(\frac{\eta_{\max}}{\eta - \eta_0}\right)^{\lambda_c} \quad (2.16)$$

where,  $\lambda_c = 0.2$  and  $\zeta = 1$ .

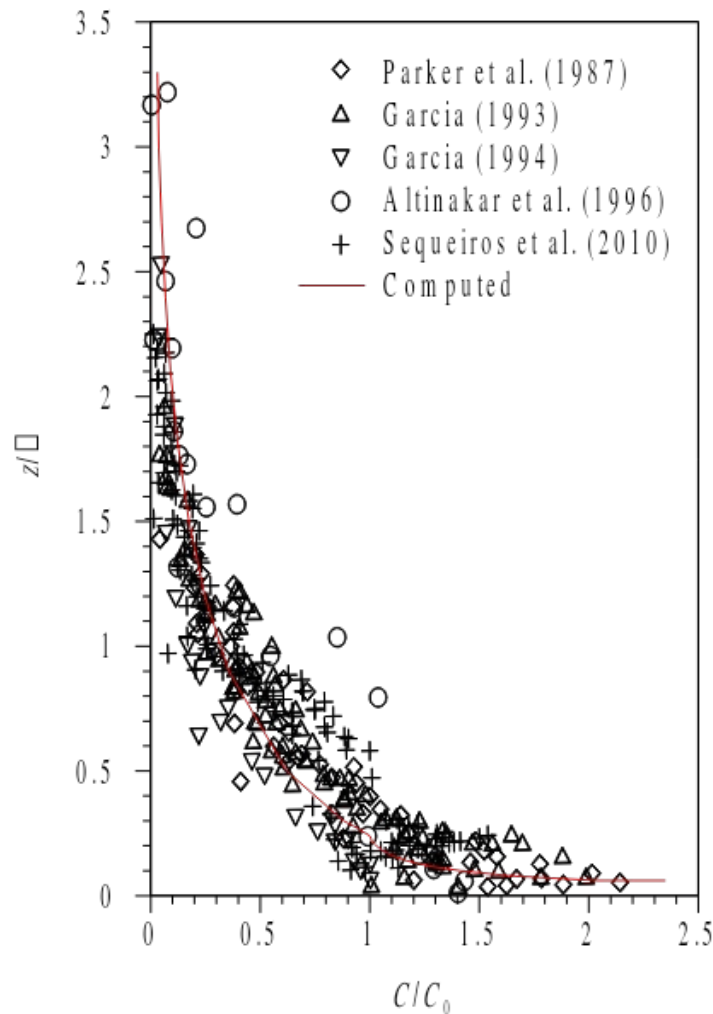


**Fig. 2.3** Computed dimensionless concentration profiles

Fig. 2.3 presents the computed concentration distributions obtained from Eq. 2.14. The experimental data of Parker et al. (1987), García (1993, 1994), Altinakar et al. (1996), and Sequeiros et al. (2010) for gravity currents are shown in Fig. 2.3 for comparison.

## 2.5 Conclusion

The equations for velocity and concentration distributions for the near boundary and jet region are separately computed and compared with the results of previous investigators. The dimensionless profiles of velocity and of concentration are shown in Fig. 2.2 and 2.3. The modified equations gives best fit compared to the other.

## References

- Akiyama, J. and Stefan, H. (1986). Turbidity current with erosion and deposition. *Journal of Hydraulic Engineering*, 111 (12), 1473–1496.
- Altinakar, M. S., Graf, W. H., and Hopfinger, E. J. (1996). Flow structure in turbidity currents. *Journal of Hydraulic Research*, 34 (5), 713–718.
- Cantero-Chinchilla, F. N., Dey, S., Castro-Orgaz, O., and Ali, S. Z. (2015). Hydrodynamic analysis of fully developed turbidity currents over plane beds based on self-preserving velocity and concentration distributions. *Journal of Geophysical Research: Earth Surface*, 120(7), 2076-2199.
- Dey, S., Nath, T. K. and Bose, S. K. (2010). Submerged wall jets subjected to injection and suction from the wall. *Journal of Fluid Mechanics*, 653, 57–97.
- Ellison, T. H. and Turner, J. S. (1959). Turbulent entrainment in stratified flows. *Journal of Fluid Mechanics*, 6 (3), 423.
- Garcia, M. H. (1993). Hydraulic jumps in sediment-driven bottom currents. *Journal of Hydraulic Engineering*, 119 (10), 1094–1117.
- Garcia, M. H. (1994). Depositional turbidity currents laden with poorly sorted sediment. *Journal of Hydraulic Engineering*, 120 (11), 1240–1263.
- Lee, H.Y. and Yu, W.S. (1997). Experimental Study of Reservoir Turbidity Current. *Journal of Hydraulic Engineering*, 123 (6), 520–528.
- Parker, G., Fukushima, Y. and Pantin, H. M. (1986). Self-accelerating turbidity currents. *Journal of Fluid Mechanics*, 171 (1), 145.
- Parker, G., Garcia, M., Fukushima, Y. and Yu, W. (1987). Experiments on turbidity currents over an erodible bed. *Journal of Hydraulic Research*, 25 (1), 123–147.
- Sequeiros, O. E., Spinewine, B., Beaubouef, R. T., Sun, T., García, M. H. and Parker, G. (2010). Characteristics of Velocity and Excess Density Profiles of Saline Underflows and Turbidity Currents Flowing over a Mobile Bed. *Journal of Hydraulic Engineering*, 136 (7), 412–433.
- Stacey, M. and Bowen, A. (1988). The vertical structure of density and turbidity currents: theory and observations. *Journal of Geophysical Research*, 93, 3528–3542.

# 3

## Scour due to Offset Jets

### 3.1 General

The scour is a result of the erosive action of flowing water, excavating and carrying away material from the bed and banks of streams and from around the piers and abutments of bridges. Such scour around pier and pile supported structures and abutments can result in structural collapse and loss of life and property. Local scour (also termed localized scour) is developed near the structures due to modification of the flow field as a result of obstruction to the flow by the structures. Scour within the contracted portion of rivers, scour downstream of structures, scour at bed sills, scour below horizontal pipelines, scour at bridge piers and abutments, and scour at other river training works are the examples of local scour. It is very important to reduce local scour caused by impacting jets. Scour downstream of an apron due to jet issuing from a sluice opening is important from the point of view of the stability of hydraulic structures. The scour phenomenon downstream of a sluice gate opening is complex in nature owing to the abrupt change of the flow characteristics on the sediment bed (Dey and Sarkar 2006a). Scouring of bed in the downstream of any hydraulic structure, spillways, downstream of spurs in a river, diffusors (very often multiple jets), and propeller jets of ships hydraulic structures is mainly caused by the freely falling jets. Scour due to jets occurs very rapidly, which causes danger to the stability of the channel bed, in addition to the devastating effects. At hydraulic structures, it is normally desirable to dissipate the energy of the jet in order to limit scour. Therefore, relatively high tailwater conditions often exist, together with hydraulic jump formation and jet discharge under submerged conditions.

A forceful stream of fluid (water or gas) discharged from a narrow opening or a nozzle is called a jet. Jet fluid has a higher momentum compared to the surrounding fluid medium. In the case where the surrounding medium is made up of same fluid as the jet

and this fluid has a viscosity, than the surrounding fluid near the jet is assumed to be carried along with the jet by a process called entrainment. When excess water is discharged from a reservoir into the downstream water body, it often flows in the form of a jet. This high energy water jet can pick up sediment particles and transport them downstream of the impinging area, thereby forming a scour hole that may affect the stability of the upstream structure.

Jet flow may be two-dimensional or three-dimensional, free or submerged depending on the tailwater depth (Chiew and Lim, 1996). Depending on the location of the jet relative to the undisturbed bed level, it can be a wall jet or an offset jet. Scour induced by submerged offset jets can be found near sewage outfall Fig. 3.1 (a) and the downstream sluiceway of dam Fig. 3.1(b).

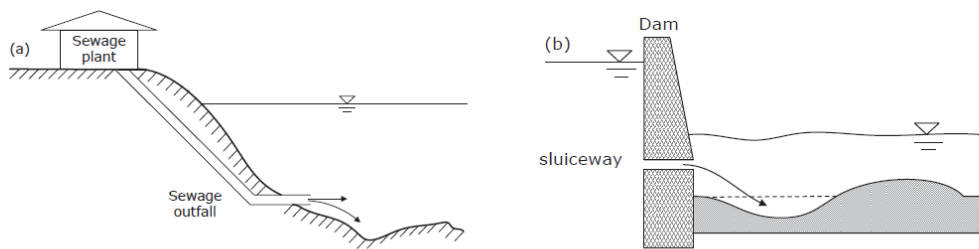


**Fig. 3.1** Examples for offset jets (a) schematic diagram of sewage outfall; (b) sluiceway of dam

An offset jet is a jet through which water falls from a certain height into the channel bed surrounded by the same fluid. Local scour downstream of a hydraulic structure is a common problem due to the impact of jet of water ejecting through the spillway. When excess water is discharged from a reservoir into the downstream water body, it often flows in the form of an offset jet. This high energy water jet can pick up sediment particles and transport them downstream of the impinging area, thereby forming a scour hole that may affect the stability of the upstream structure. An offset jet is formed when it flows into a downstream water body at a location above the bed level (Fig. 3.1). The flow pattern of the offset jet is complex in nature where the fluid jet issuing from a certain height above the bed level follow a reattachment to the solid boundary. The reattaching offset jet (ROJ) is also known as the Coanda jet after the Romanian aerodynamicist Henri Marie Coanda (1886–1972). The high velocity flow from a sluice gate placed over an abrupt drop forms a reattached offset jet (Rajaratnam and

Subramanya, 1968). This class of flows is important for various engineering applications such as stabilizing positions of hydraulic jumps for energy dissipation, environmental discharges including disposal of municipal or industrial wastewater, fluid injection systems, circulation controller, and modulated mixing.

Coanda effect is the phenomena in which a jet flow attaches itself to a nearby surface and remains attached even when the surface curves away from the initial jet direction. If an offset jet is discharged into a downstream pool, free shear layers are developed at the peripheral surface of the jet, and the entrainment of fluid occurs. In the case of a two-dimensional offset jet, there is reduced pressure from the bottom of the jet because of the presence of a solid boundary which results in the deflection of the jet towards that boundary. As the jet approaches the boundary, the flow decelerates, and pressure inside the jet rises. Eventually, the offset jet reattaches to the wall, enclosing a separated flow zone in which a reverse eddy is formed. Upon reattaching, the jet behaves like an impinging jet, and the pressure at the impinging zone becomes larger than hydrostatic attaining the maximum near the impinging point. The forward flow is accelerated because of the favorable pressure gradient set by the reattachment. At the end of the impingement zone, the acceleration ceases, and a turbulent wall jet condition is established. A new internal boundary layer in the forward flow is developed in this developing wall jet region, which increases in thickness because of the presence of the solid boundary and turbulent diffusion. A mixing layer is established at the upper part of this jet, and a large reverse-flow region is created near the free surface, which is significantly affected by the shallow tailwater depth. Further downstream, the velocity distributions gradually recover to the normal subcritical open-channel flow.

### **3.2 Review of Literature**

Hydraulic structures are built in rivers for various purposes like for river training works, for water storage for future use or for producing electricity and sometimes to decrease the flow velocity or sometimes to provide passage to connect the opposite banks of rivers. Due to the river bed soil and flow characteristics, it is seen that sediment is eroded and deposited at a certain distance in bed and some of the sediment particles remain suspended. As a result scouring forms. A lot of experimental work and numerical simulations on scouring due to submerged horizontal jets have been done by various researchers before, however a few has been done considering offset jet and

mathematical investigations. Here is a brief review on the work studied by them.

Rajaratnam (1981) presented the results of an experimental study on erosion caused by plane wall jets of air and water on beds of sand and polystyrene and also did the same for impinging plane jets of water and air on beds of sand. By using dimensional analysis, the characteristics features of the scoured bed in the asymptotic state were analysed. For the scour formed by wall jet, it was found that the asymptotic profile in the scour hole part is similar with the maximum depth of erosion and the distance of this section from the nozzle as the length scales. Moreover, the maximum erosion depth, its distance from the nozzle, height of the ridge formed in the downstream end of the scour hole and its distance from the nozzle in terms of the thickness of the jet are functions of densimetric Froude number. Ali and Neyshaboury (1991) studied local scour caused by deeply submerged 2D offset jets. They conducted various experiments to study the time variation of scour by changing sediment sizes, jet heights and flow velocity. They observed that the characteristics of scour depend on time, Froude number, and more importantly on sediment size and height of the jet above the bed. Moreover, at the asymptotic state, it was found that when the height of the offset jet is smaller, depth of the scour hole is more than that caused by a jet with a bigger height. They presented results of detailed experimental investigation on the behaviour of turbulent offset jet at asymptotic conditions of the scouring process but they did not perform any mathematical model to study the scour process. They measured the horizontal and vertical velocity distributions but did not explore the characteristics of velocity and turbulence in an evolving scour hole. Chatterjee et al. (1994) studied the occurrence of local scour and sediment transport formed by horizontal jet of water coming out from sluice opening. They observed that the rate of scour is relatively high in the first few minutes and goes on decreasing as the scour continues. The scour profiles are time independent and also same in nature but dependent on the characteristics of bed grain-size. The scour characteristics have been described by the time to reach the equilibrium stage, the locations of the maximum scour depth, and the locations of the peak of the dune from the end of the rigid apron. Each of these variables has successfully been expressed in terms of flow parameters and sediment characteristics. Chiew and Lim (1996) used two types of circular jets, wall jet and offset jet, having air as well as water flowing through the jet, to study local scour in uniform cohesionless sediment bed. They

performed various experiments with densimetric Froude number of 13.14 - 60.74 and offset ratio of 0.5 - 15.75. They found densimetric Froude number to be the main characteristic scouring parameter in relation with the maximum equilibrium scour dimension. They further noted that higher offset distance in an offset jet causes smaller scour hole, because the maximum flow from the jet is elevated farther away from the sediment bed, and most of the energy is diffused into the flow instead of being used to erode the sediment. They observed scouring in air jet to be sooner than that in the water jet. They did not explain the scour process by mathematical or analytical model. Sarkar and Dey (2005) experimentally studied the characteristics of scour holes downstream of an apron due to a submerged horizontal jet issuing from a sluice opening. They found that the scour profiles for scour holes downstream of the apron are nearly similar. They provided various guidelines to civil engineers for designing apron foundations and protective measures (such as launching aprons) for scour downstream of an apron in uniform and non-uniform sediments. The characteristic lengths of the scour hole were determined from the scour profiles. They found that for non-uniform sediments the horizontal distance of the dune crest from the edge of the apron, the dune height, the horizontal distance of maximum scour depth from the edge of the apron, the horizontal extension of scour hole from the edge of the apron and the maximum equilibrium scour depth all decrease with increases in geometric standard deviation of sediments and for uniform sediments, the horizontal distance of the dune crest from the edge of the apron, the horizontal distance of maximum scour depth from the edge of the apron, the horizontal extension of scour hole from the edge of the apron and the maximum equilibrium scour depth were all found to increase with increase in densimetric Froude number, whereas the dune height decreases with increase in densimetric Froude number.

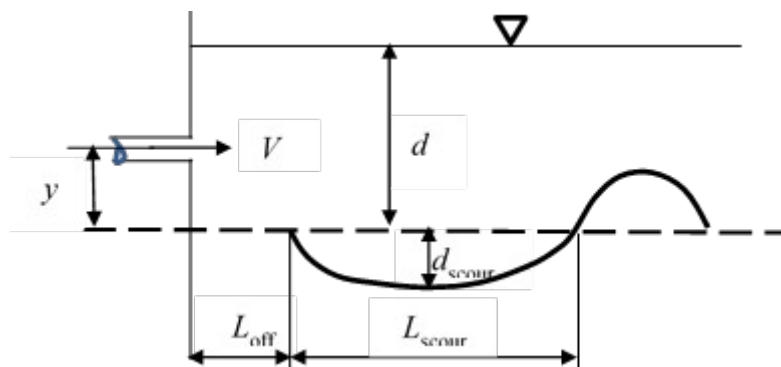


**Fig. 3.2** Scour by a deeply submerged circular offset jet. (Chiew and Lim, 1996)

Faruque et al. (2006) studied scour caused by three-dimensional jets issuing from a square cross-section nozzle on to a non-cohesive sand bed and performed experiments using two different nozzles and three tailwater depths. The densimetric Froude number was maintained below 10, while the jet expansion ratio was held greater than 10. The results indicate that the densimetric Froude number, tailwater depth, and grain size-to-nozzle width ratio, all have an influence on the extent of scour and each parameter has a dominant influence at different flow conditions. They observed that at lower values of densimetric Froude numbers (<5), non-dimensional tailwater depth and grain size-to-nozzle width ratio have no effect on the maximum depth of scour whereas at higher densimetric Froude numbers, the effect of tailwater depth appears to be important at larger values of grain size-to-nozzle width ratio. A set of scaling parameters based on nozzle hydraulic radius, grain size, and densimetric Froude number provided a better scaling of the time variation of the scour parameters. Dey and Sarkar (2006) performed number of experiments on scour in uniform and non-uniform cohesionless sediment beds downstream of an apron by submerged horizontal jet discharging from a sluice opening, for various sluice openings, jet velocities, apron lengths, and tailwater depths. They found that the scour profiles follow a particular geometrical similarity at different times, and is expressed by a combination of two polynomials,

$$\hat{y}(\hat{y} \leq 0) = a_0 + a_1 \hat{x} + a_2 \hat{x}^2 + a_3 \hat{x}^3 \quad (3.1)$$

$$\hat{y}(\hat{y} > 0) = b_0 + b_1 \hat{x} + b_2 \hat{x}^2 + b_3 \hat{x}^3 \quad (3.2)$$

where,  $a_{0-3}$  and  $b_{0-3}$  are coefficients obtained from scour profiles and boundary conditions. The time variation of scour depth increases linearly with densimetric Froude number. The equilibrium scour depth increases as apron length, sediment size and sluice opening decreases, and increases with increase in densimetric Froude number. Experiments were performed with various densimetric Froude number ranging from 5.7 to 12.61. The equilibrium scour time considered in this study is 12h. The maximum equilibrium scour depth as measured in this work lies in the range of  $6.57 \leq \hat{h} \leq 13.85$  and  $\hat{l} > 26$  where  $\hat{h} = h/b$  and  $\hat{l} = l/b$  and  $l$  = apron length and  $b$  = sluice gate opening. Dey and Raikar (2007) conducted various experiments and

analysed the results on scour below a high vertical drop using uniform sand and gravel. They found that the parameters influencing the equilibrium scour depth below a vertical drop are tailwater depth, jet thickness, and velocity of jet, mass density of water, mass density of sediments, gravitational acceleration, and kinematic viscosity of water. They observed that the equilibrium scour depth increases with increase in densimetric Froude number, whereas the scour depth decreases with increase in sediment size and tailwater depth. To represent the time variation of scour depth, the time scale that follows an exponential law is obtained. Karki, Faruque, and Balachandar (2007) used both square and 2D offset jet to perform experimental study of scour process. The square offset jet test is performed for densimetric Froude number 10 and deep tail water depth while the 2D offset jet test is conducted for 5.5 and 10 densimetric Froude number considering both shallow and deep tail water depth conditions. They found that for both the types of jets for a given densimetric Froude number, depth of the scour hole decreases and total length increases as offset distance increases. Moreover, the time required for the initiation of significant scour increases with increase in offset distance for both types of offset jet. They observed that the offset distance is the most important factor affecting scour in addition to other geometric parameters for both jets. They did not perform mathematical model to study the scour process. They did not explore the characteristics of velocity and turbulence in an evolving scour hole. Dey and Sarkar (2008) using acoustic Doppler velocimeter performed an experimental investigation on the velocity and turbulence characteristics in a scour hole produced downstream of an apron caused by submerged jets emerging from a sluice opening. Experiments were carried out with jet Froude numbers ranging from 2.58 to 4.87 and submergence factors 0.96 to 1.85. The important interpretations they made about the flow characteristics in submerged jet are: the flow in the fully developed zone is self-preserving over apron and scoured bed, local maximum horizontal velocity decay rate increases with an increase in scour hole dimension, horizontal velocity's inner-layer thickness and turbulence intensity distributions increases due to bed roughness and scour hole, the decay rate of the local maximum Reynolds stress, horizontal, and vertical turbulent intensities over scoured beds are slower than those over the apron. They also found that the decay rate of local maximum horizontal velocity increases with an increase in scour hole dimension. Chiew et al. (2012) collected experimental data of

offset and propeller jet scour from published literature to investigate the characteristics of the scour hole formed on a uniform cohesionless sediment bed and found that the densimetric Froude number  $F_0$  and the offset height are the two primary parameters in affecting the scour hole dimensions. They found the dimensionless scour depth is directly proportional to densimetric Froude number and inversely proportional to dimensionless offset height, and dimensionless scour length and dimensionless scour width, both are directly proportional to Froude number and dimensionless offset height. Hong et al. (2012) experimentally investigated the evolution of scour caused by propeller jet. They observed that the equilibrium scour profile comprises of three components- a small scour hole directly beneath the propeller; a primary scour hole downstream of the small scour hole; and a sand dune farther downstream of the primary scour hole and also examined the similarities and differences that exist in the equilibrium scour profile developed under different conditions. They proposed a semi-empirical formula based on the densimetric Froude number, offset height and a reference time scale, to simulate the temporal development of the maximum scour depth that showed good agreement with the experimental data. Hong, Chiew, and Cheng (2013) investigated the development of a scour hole with non-cohesive sediments due to the jet induced by a rotating propeller. They conducted experiments with sediment particles of median size 0.34 - 1.46, densimetric Froude number of 6.08 - 10.69 and offset ratio of 0.5 - 1 and tailwater depth of 0.45 m and 0.6 m for a time period of 64h. Dimensionless equation for the estimation of time dependent scour depth induced by a propeller wash is developed and its simulated results compared well with the experimental data used in the paper and those from the published literature. The time to initiate propeller scour decreases with decreasing densimetric Froude number and propeller diameter but increases with increasing sediment size and offset height. The densimetric Froude number and the offset ratio play the most important role in affecting the scour dimensions caused by both offset and propeller jet. The wall jet induces the deepest scour depth for the same value of densimetric Froude number than that of the offset jets and propeller jets. They developed an equation that can be used to account for the scour depth induced by an offset and a propeller jet and to deduce the critical condition for the initiation of scour.

$$13 \frac{d_{s,me}}{d_0} = 0.265 \left[ F_0 - 4.114 \left( \frac{y_0}{d_0} \right) \right]^{0.955} \left( \frac{y_0}{d_0} \right)^{-0.022} \quad (3.3)$$

$$\text{where } \left( \frac{y_0}{d_0} \right) \geq 0.5$$

$d_{s,me}/d_0$  = dimensionless scour depth;  $F_0$  = densimetric Froude number;  $y_0/d_0$  = offset ratio.

Melville and Lim (2014) analysed 309 known laboratory data for local scour depth developed by two-dimensional horizontal jets, which leads to development of a new comprehensive prediction equation that comprises a number of mutually independent multiplying factors, which account for the effects on local scour depth of the characteristics of the applied jet flow and the bed sediment, as well as the extent of a downstream protective apron. When utilized in terms of the jet thickness, the equation shows that the maximum possible dimensionless local scour depth is equal to three times the jet Froude number expressed in terms of jet velocity and jet thickness. The equation is compared to most of the existing predictive equations by applying each equation to the existing data, the comparison indicating that the new method has superior performance. Indeed, many of the existing predictive equations are shown to perform poorly when judged against the known laboratory data. They gave the following equation for prediction of local scour depth due to 2D horizontal jets that performs better than existing predictive equations, when judged against the known laboratory data.

$$\frac{y_s}{y_j} = 3F_j K_D K_{yt} K_\sigma K_L \quad (3.4)$$

where  $F_j$  = strength of the applied flow;  $y_s$  = local scour depth;  $y_j$  = thickness of jet at vena-contracta; the  $K$ s are dimensionless multiplying factors expressing the influence on scour depth of sediment size ( $K_D$ ), tail water depth ( $K_{yt}$ ), sediment gradation ( $K_\sigma$ ), and apron length ( $K_L$ ).

Most of the researchers explained only the dependency of various parameters on the scour caused by the offset jet from visual observations and simple calculations. The results of detailed experimental investigation on the behaviour of offset jet at asymptotic conditions of the scouring process were investigated but they did not

perform any mathematical model to study the scour process. The horizontal and vertical velocity distributions were measured at various locations but the characteristics of velocity and turbulence in an evolving scour hole were not explored.

### 3.3 Parameters related to scour

1. Bed Sediment-median size ( $d_{50}$ ), grain size distribution(S-curve), cohesiveness, relative density, angle of repose, thickness of the sediment bed ( $t$ ).

**Table 2.1: Characteristics of Sediments Used in the Experiments**

Median size( $d_{50}$ )	Angle of Repose( $\varphi$ )	Relative density( $s$ )	Geometric standard deviation
1.81 mm	31.9	2.65	1.28

where,  $d_{50}$  is the 50% finer sediment size.

#### 2. Flow parameters-

- Width of the flume at the sluice gate opening ( $B = 6\text{cm}$ ),
  - Offset height,  $h$  (variable),
  - Sluice gate opening ( $b = 4\text{cm}$ ),
  - Jet Froude number [ $F_r = U/(gb)^{0.5}$ ],
  - Densimetric Froude number [ $F_0 = U/(\Delta g d_{50})^{0.5}$ ],
  - Velocity at the gate opening [ $U = F_r \times (gb)^{0.5}$ ],
  - Discharge [ $Q = U \times B \times b$ ]
  - Offset distance ratio =  $h/b$
  - Tailwater depth
3. Time of scour can be taken as an additional parameter ( $T = 10\text{-}12$  hrs)
  4. Fluid: Mass density ( $10^3 \text{ kg m}^{-3}$ ), viscosity (approximately  $10^{-6} \text{ m}^2 \text{ s}^{-1}$  at  $20^\circ \text{C}$ ), gravitational acceleration ( $g = 9.81 \text{ m s}^{-2}$ ), and temperature

### 3.4 Experimental Setup and Procedure

The laboratory experiments were carried out in a flume, having cross section of 0.6 m wide, 0.71 m deep and 10 m long, at the Hydraulic and Water Resources Engineering Laboratory, Department of Civil Engineering, Indian Institute of Technology, Kharagpur, India as shown in Fig. 3.3. The transparent sidewalls of the flume allowed optical access. A sediment recess of 0.6 m width and 2 m long and depth 0.3 m was prepared based on

few trial runs and levelled to the required offset distance. The test section was located 5 m from the upstream end of the flume. Two small holes were provided at the bottom of the downstream wall of the sediment recess to drain out water at the end of the experiment. A sediment trap was constructed adjacent to the downstream wall of the sediment recess to prevent the scoured sediments to go into the underground reservoir. There was an inclined concrete stilling basin consisting of one baffle wall and two vertical steel screens at the inlet of the flume through which water entered into the flume. The apron of height 0.3 m was made of Perspex sheet over which vertical sluice gate was fixed. A Perspex vertical sluice gate, which had a streamlined lip to produce a supercritical flow with a thickness equal to the gate opening, was fitted over the bed. Sediments samples of median size  $d_{50} = 1.81$  mm was prepared for using in the experiments. The Indian Standard sieves were used for the preparation of different samples. The data of sieve analysis were plotted to draw the particle size distribution curves and  $d_{50}$  was obtained from the curves for the sediment sample. The properties of sands and gravels used in the experiments are summarized in Table 2.1. The depth of sediment recess was adjusted depending on the required offset ratio. A Vernier point gauge with an accuracy of  $\pm 0.1$  mm was used to measure the flow depths. An adjustable tailgate in the downstream of the flume controlled the tailwater depth in the flume. The water supply system consists of a constant head reservoir, an inlet tank, pumps and a large underground reservoir. A valve was fitted at the junction of constant head reservoir and inlet tank regulated the water supply in the inlet tank. The water discharge at the inlet, controlled by an inlet valve, was measured by a calibrated V-notch weir. A few experiments were carried out to investigate the effect of various parameters on the equilibrium scour depth.

The sluice gate was placed over the apron and was adjusted to have the required gate opening of 0.02 m and different sluice gate openings can be changed by adjusting the gate vertically over the smooth apron. The sediment bed was levelled properly with sediment size of  $d_{50} = 1.81$  mm and was checked by using a Vernier point gauge before starting the experiments. The final bed level was also checked by flooding the sediment recess. The point gauge was attached to the instrument carriage which could be moved horizontally and transversely. The flume was initially filled with water at a low rate in order to avoid too much scouring of the sediment bed by the sudden action of the offset

jet issuing from the sluice gate opening. The densimetric Froude number was fixed by conducting many trial experiments using different sediment sizes, different tailwater depths and various offset ratio. The experiment was then started by adjusting the discharge to the desired value after the water level reached the desired depth. Discharge was measured using a V-notch weir and expressed as a function of head of water  $H$  above the sill level of the V-notch as:

$$Q = 0.9174H^{2.159} \quad (3.5)$$

The discharge into the flume was regulated by a valve fitted at the junction of the constant head reservoir and the inlet tank. The water level was measured by a vernier point gauge having an accuracy of  $\pm 0.1$  mm, placed at the inlet tank. The scour profiles at regular intervals of time were traced on a transparent perspex sheet attached to the outside glass wall. The perspex sheet had square grids of size 1 cm  $\times$  1 cm, facilitating reproduction of scour profiles. The runs were taken for a period of 10 to 12 h when the equilibrium scour depth was obtained. Finally, water was drained out slowly by opening the holes at the bottom of the downstream wall of sediment recess, sediment trap and tail gate.

Velocity and turbulence profiles were measured by a SonTek 5 cm down looking acoustic Doppler velocimeter (ADV), which had a sampling rate and volume of 50 Hz and 0.09 cm<sup>3</sup> respectively. A spike removal algorithm filtered the output data from the ADV. The ADV measurements were taken in the vertical plane of symmetry (VPS) along vertical lines at different streamwise distances. In order to check the two-dimensionality of the flow, the ADV measurements were also taken in other vertical planes at a transverse distance of 10 cm from either side of the VPS. The velocity profiles in these planes revealed that in the central part of the flume, the flow was reasonably two-dimensional. The acoustic beams were sent out with a frequency of 16 MHz from the transmitting transducer traveling through the water arriving at the measuring point 5 cm below the transducer, where they were reflected by the ambient particles within the flow and received by the receiving transducers. Since the measuring location was 5 cm below the ADV probe, the captured data were free from an artifact of the ADV. In the near-bed region, the recorded velocities might contain spikes are possibly due to the interference between incident and reflected pulses. The measurement by the ADV probe was not feasible in the zone located 5 cm below the free

surface. Depending on the turbulence intensity, the sampling durations was 4 minutes in order to have a statistically time-independent average velocity. Near the bed, the sampling durations were relatively long. An inbuilt acoustic device of the ADV indicated the vertical locations of the ADV measurements with respect to the bed. The closest vertical spacing of the ADV measurements was 0.2 cm. It was mainly maintained from the bed to the point of flow reversal in the fully developed zone. On the other hand, the closest horizontal spacing of the ADV measurements was 2 cm from the sluice opening to the junction of the fully developed zone and the recovering zone.

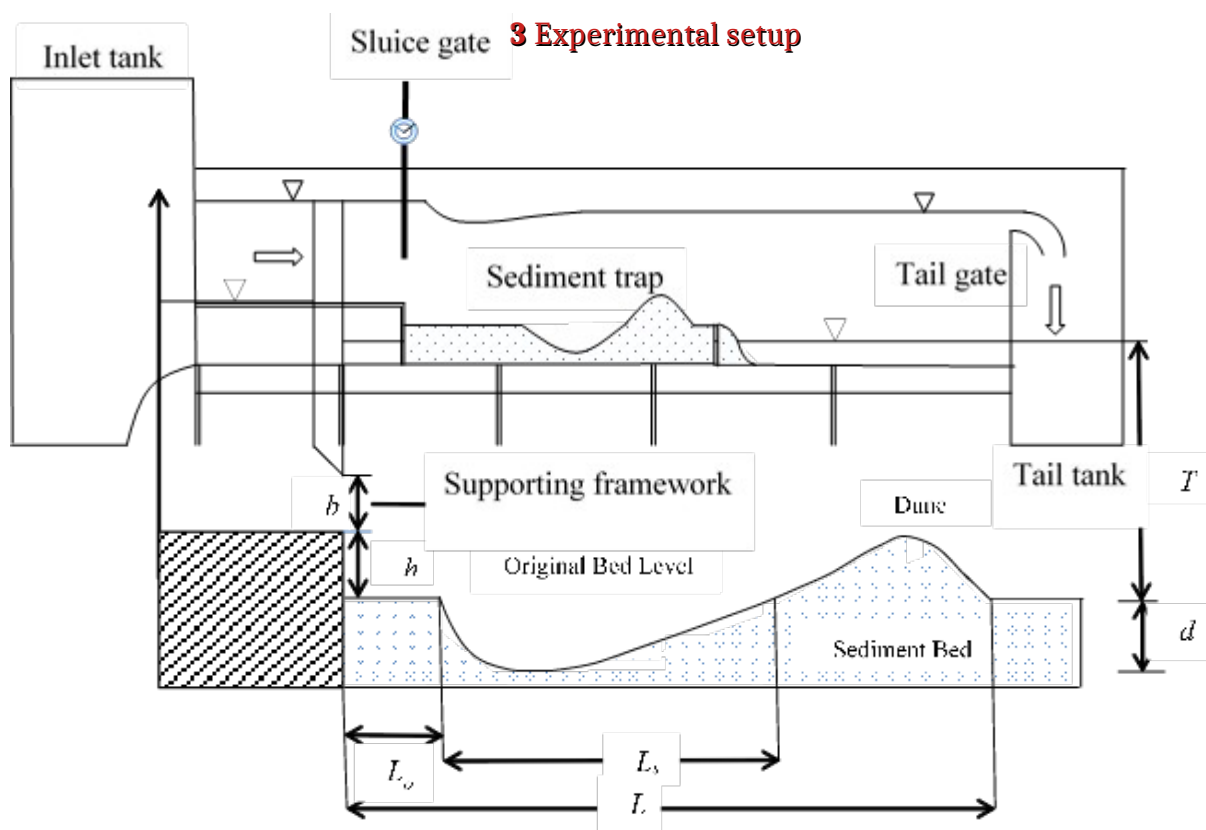


**Fig. 3.4** Schematic diagram of scour hole due to offset jet

### 3.5 Scouring Process

The scouring process due to offset jet is complex, owing to the interaction between the jet and the resistance of the bed sediment. The evolution of a typical scouring profile along the longitudinal direction may be divided into four stages:

1. **Initial stage:** During the initial stage, as flow started a main or primary scour hole is formed downstream of the apron. The scour hole grew longitudinally with the

formation of a small dune or deposition overlaid by smaller ripples. At this stage the finer particles moved away from the bed as suspended load.

2. **Developing stage:** During the developing stage, the size of the primary scour hole increased with time. As the flow separation took place at the edge of the apron having a reattachment of flow at the deepest point of the scour hole, the movement of the sediment particles was divided into two parts. Some amount of sediments moved along the downstream slope of the scour hole and ultimately went out of the scour hole. The other part was moved back along the upstream slope of the scour hole by the reversed flow and a second small dune is formed. The larger dune moved horizontally downwards away from the apron with the passage of time and the size of dune also increased.
3. **Stabilization stage:** During the stage of stabilization, the size scour holes and dunes slowly increased with time with the movement of very few sediment particles.
4. **Asymptotic stage:** After 24 h of testing, scour hole and dunes reached the asymptotic stage where no particles were in suspension. Beyond this time, the dimension of the scour hole essentially remains unchanged.

**Table 3.2: Experimental Parameters for sediment size 1.81mm**

No.	<i>B</i> (cm)	<i>t</i> (cm)	<i>l</i> (cm)	OR	OR <sub>m</sub>	<i>F<sub>u</sub></i>	<i>U</i> (m/s)	<i>Q</i> (m <sup>3</sup> /s)	<i>H</i> (cm)	<i>d</i> <sub>50</sub> (mm)	<i>F<sub>o</sub></i>	<i>T</i> (cm)
1	2	17.5	12.5	6.25	6.75	2.62	1.165	0.0139	30	1.81	6.81	61.5
2	2	17.5	12.5	6.25	6.75	2	0.886	0.0106	30	1.81	5.17	61.5
3	2	17.5	12.5	6.25	6.75	2.3	1.018	0.0122	30	1.81	5.95	61.5

### 3.6 Scour Profiles

The evolving scour hole at any time follows a particular profile as given in Fig. 3.4. Typical scour profiles at different times during the development of the scour hole for different Froude numbers are shown in Fig. 3.5, 3.6 and 3.7. It is observed that an existence of a similarity of the scour profiles can be established by plotting the profiles in dimensional coordinates *xy*, where *x* is the horizontal distance; *y* = vertical distance;

and  $d_{se}$  is the maximum scour depth at any time  $t$ . It is found that the maximum scour depth increases with increase in Froude number.

### 3.7 Distributions of Velocity profiles

Fig. 3.4 describes a schematic diagram of scour downstream of an apron due to submerged offset jet issuing from a sluice opening. The velocity distribution in the region from the starting of scour hole to the end of dune was investigated for different times at different longitudinal distances using ADV. The velocity measurements were obtained at eight different locations downstream of the nozzle along the centreline of the nozzle. Fig. 3.8, 3.9 and 3.10 shows the velocity distributions at different stages of scour process. Fig. 3.8 shows the vertical distributions of streamwise velocity  $u$  for intermediate scour hole of  $0.3d_{se}$ , Fig. 3.9 shows the vertical distributions of  $u$  for intermediate scour hole of  $0.7d_{se}$  and Fig. 3.10 the vertical distributions of  $u$  for equilibrium scour depth. The maximum scour depth,  $d_{se}$  is 12.5 cm, 30% of scour depth is 3.75 cm and 70% of the scour depth is 8.75 cm. There is a negative velocities or the reverse-velocity in the surface. The presence of a solid boundary results in the deflection of the jet towards that boundary, thus the offset jet reattaches to the wall, enclosing a separated flow zone in which a reverse eddy is formed. At the end of the recirculation region is the reattachment region where the pressure becomes larger than hydrostatic attaining the maximum near the reattached point. The forward flow is accelerated because of the favourable pressure gradient set by the reattachment. At the end of the reattached zone, the acceleration decreases, and a turbulent wall jet condition is established. Further downstream, the velocity distributions gradually recover to the normal subcritical open-channel flow.

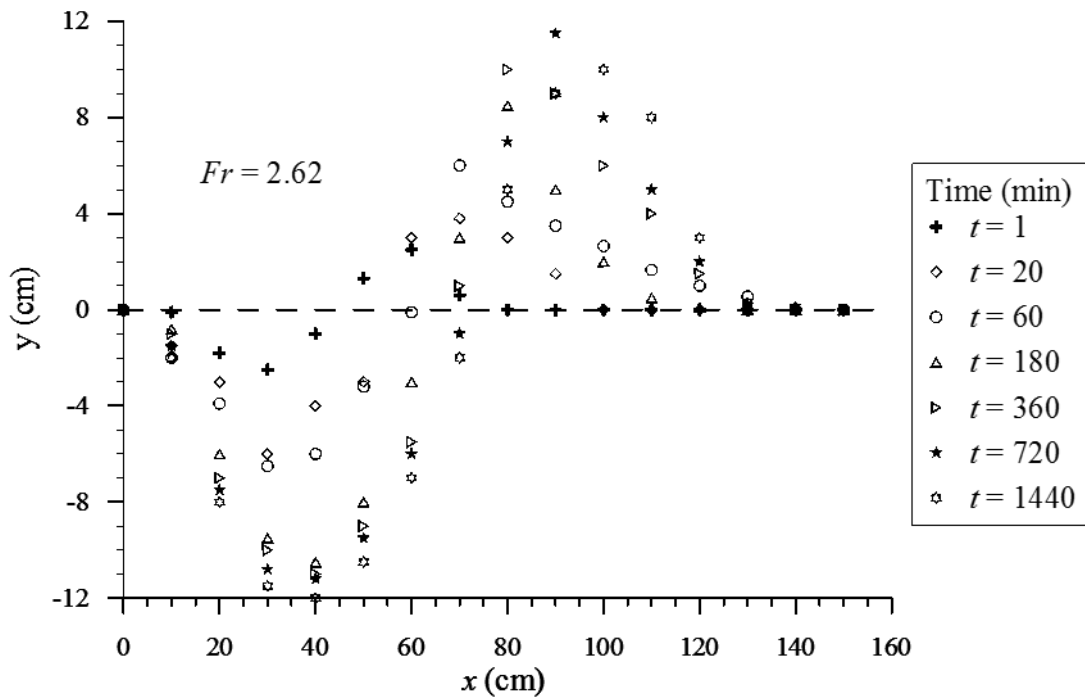


**Fig. 3.5** Scour profiles at different times for Froude number 2.62

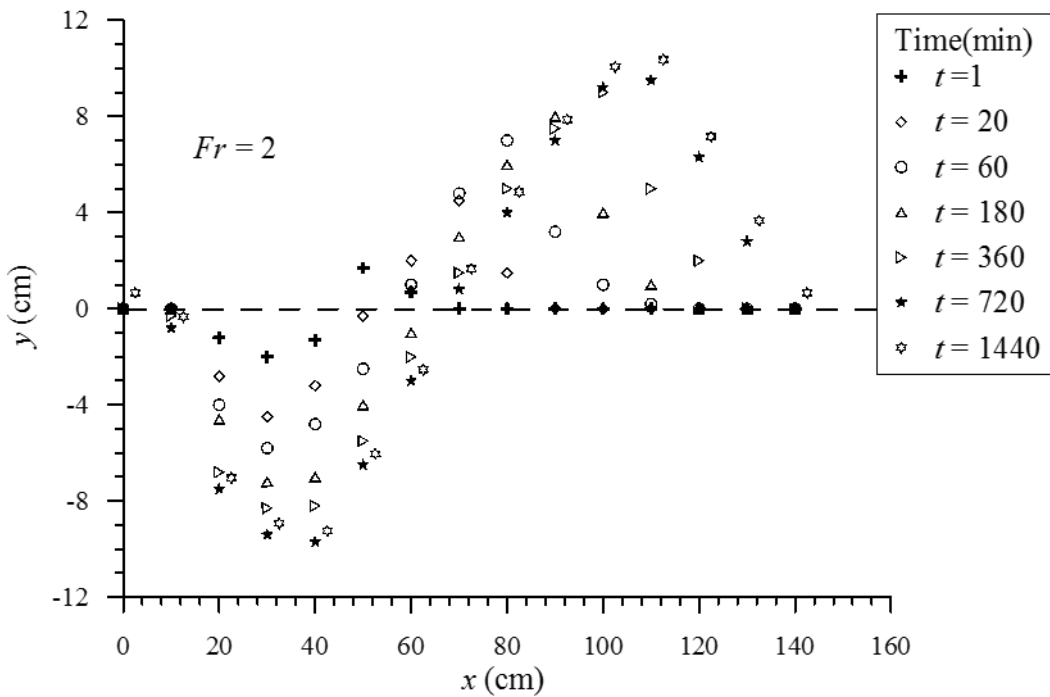


**Fig. 3.6** Scour profiles at different times for Froude number 2

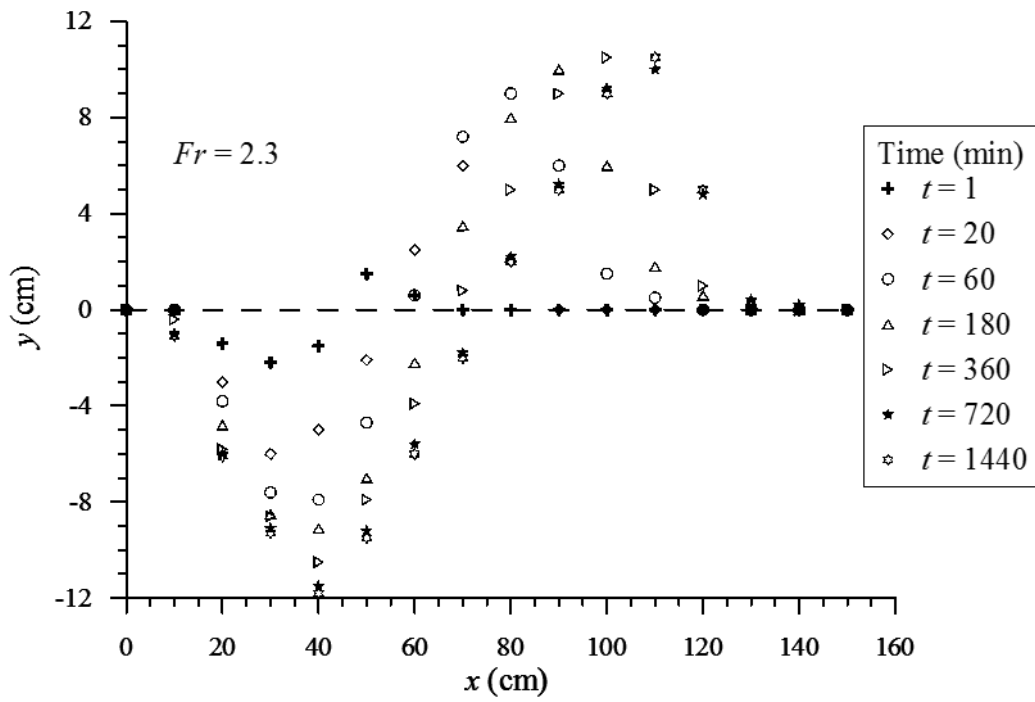


**Fig. 3.7** Scour profiles at different times for Froude number 2.3

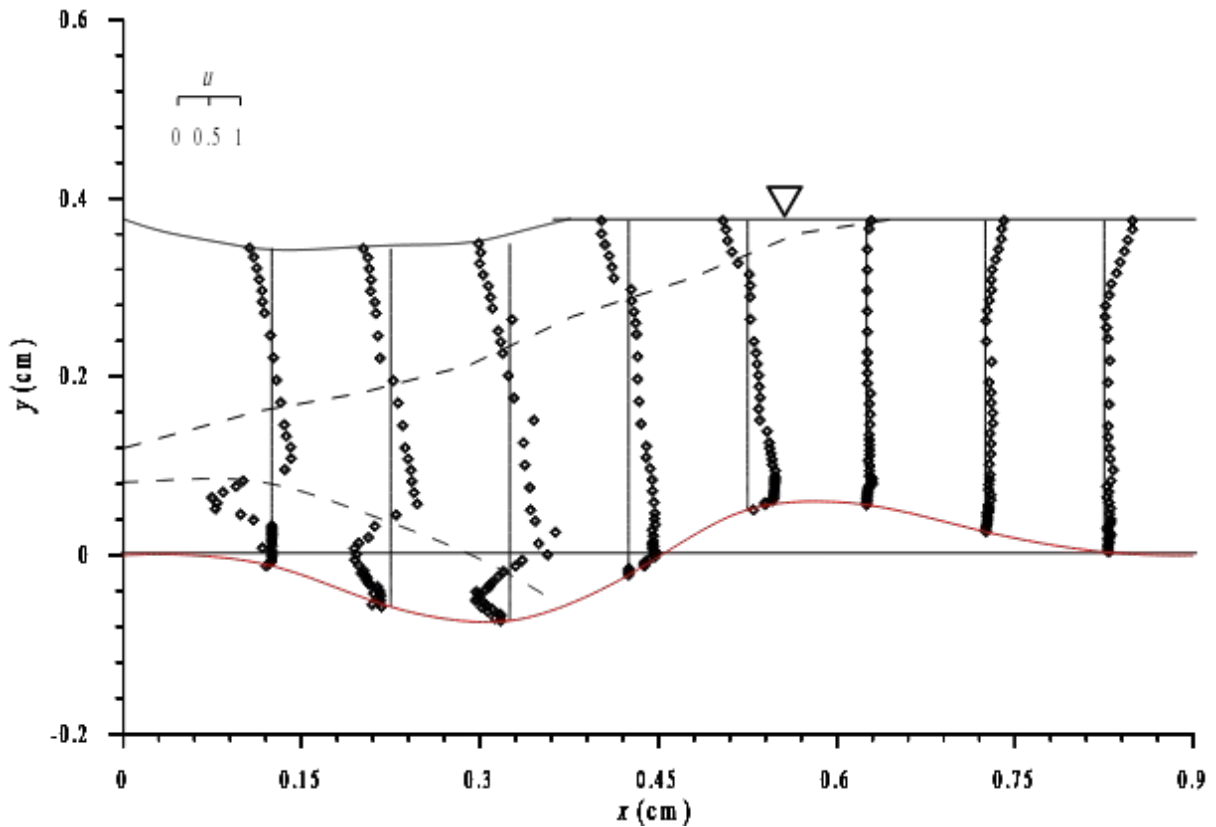


**Fig. 3.8** Vertical distributions of  $u$  for intermediate scour hole of  $0.3d_{se}$

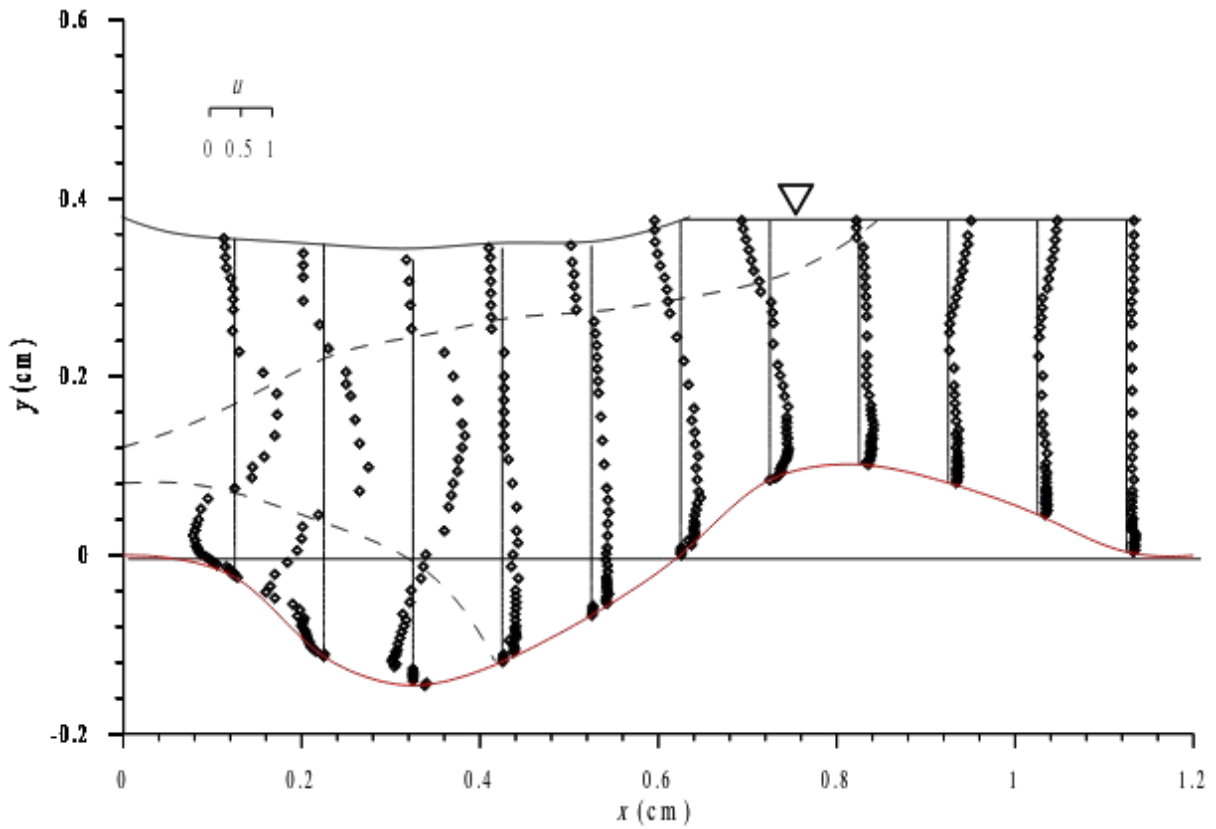


**Fig. 3.9** Vertical distributions of  $u$  for intermediate scour hole of  $0.7d_{sc}$

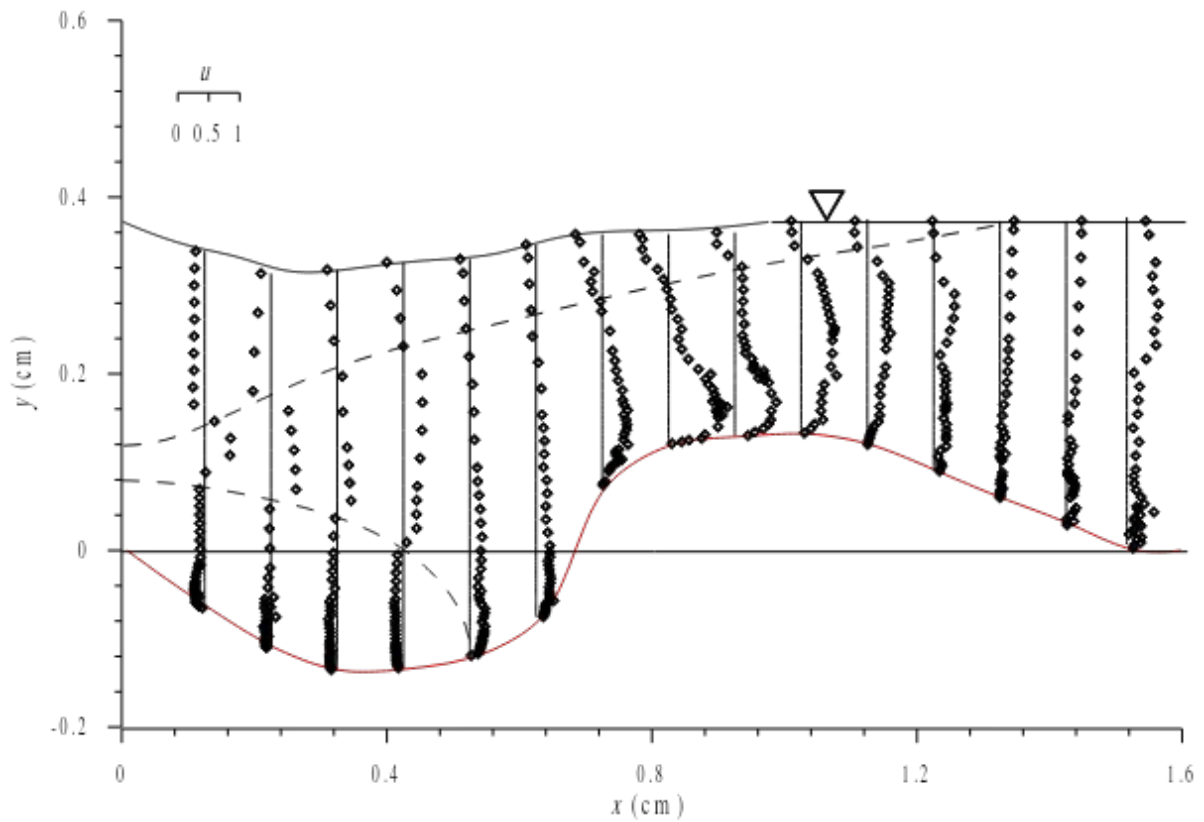


**Fig. 3.10** Vertical distributions of  $u$  for equilibrium scour depth

### 3.8 Conclusions

1. The maximum depth of scour increases with increase in densimetric Froude number.
2. The maximum width of the scour hole was wider and its location was closer to the nozzle with decreasing offset distance.
3. The depth of scour hole decreases with increase in sluice gate opening.
4. The scour profiles at different time follow a geometrical similarity.
5. The vertical distributions of time-averaged velocity components, at different streamwise distances from the sluice opening have been presented. The flow is found to be self-preserving in general. The decay rate of local maximum horizontal velocity increases due to bed roughness.

### References

- Adduce, C. and Sciortino, G. (2006). Scour due to a horizontal turbulent jet: Numerical and experimental investigation. *Journal of Hydraulic Research*, 44 (5), 663–673.
- Bhuiyan, F., Habibzadeh, A., Rajaratnam, N. and Zhu, D. Z. (2011). Reattached Turbulent Submerged Offset Jets on Rough Beds with Shallow Tailwater. *Journal of Hydraulic Engineering*, 137, 1636–1648.
- Rajaratnam, N. (1981). Erosion by plain turbulent jets. *Journal of Hydraulic Research*, Delft, The Netherlands, 19 (4), 339-358.
- Ali, K.H.M. and Salehi Neyshaboury, A.A. (1991). Localized scour downstream of a deeply submerged horizontal jet. *Proceedings of Institution of Civil Engineers, Part 2*, 91 (1), 1- 18.
- Chiew, Y.M. and Lim, S.Y. (1996). Local scour by a deeply submerged horizontal circular jet. *Journal of hydraulic Engineering, A.S.C.E.*, 122 (9), 529-532.
- Chatterjee, S. S., Ghosh, S. N. and Chatterjee, M. (1994). Submerged horizontal jet over erodible bed. *Journal of Hydraulic Division*, 106 (11), 1765–1782.
- Dey, S. and Sarkar, A. (2006). Scour downstream of an apron due to submerged horizontal jets. *Journal of Hydraulic Engineering, A.S.C.E.*, 132 (3), 246-257.
- Dey, S. and Raikar, R.V. (2007b) Scour below a high vertical drop. *Journal of Hydraulic Engineering*, 133 (5), 564–568.

- Dey, S. and Sarkar, A. (2008). Characteristics of Submerged Jets in Evolving Scour Hole Downstream of an Apron. *Journal of Engineering Mechanics*, 134 (11), 927–936.
- Faruque, M. A. A., Sarathi, P. and Balachandar, R. (2006). Clear Water Local Scour by Submerged Three-Dimensional Wall Jets: Effect of Tailwater Depth. *Journal of Hydraulic Engineering*, 132 (6), 575–580.
- Hong, J.H., Chiew, Y.M., Susanto, I. and Cheng, N.S. (2012). Evolution of scour induced by propeller wash. Submitted to the 6th International Conference on Scour and Erosion, Paris.
- Hong, J.H., Chiew, Y.M. and Cheng, N.S. (2013). Scour Caused by a Propeller Jet. *Journal of Hydraulic Engineering*, 139(9), 1003–1012.
- Karki, M.A.A., Faruque, M.A.A. and Balachandar, R. (2007). Local scour by submerged offset jets. *Proceedings of Institution of Civil Engineers, Water Maritime and Energy*, 160 (3), 169-179.
- Melville, B. W. and Lim, S.Y. (2014). Scour Caused by 2D Horizontal Jets. *Journal of Hydraulic Engineering*, 140 (2), 149–155.
- Sarkar, A. and Dey, S. (2005). Scour downstream of aprons caused by sluices. *Proceedings of Institution of Civil Engineers, Water Maritime Energy*, 158, 55–64.

© MultiSpectra Consultants, 2019.